Annals of Biomedical Engineering, Vol. 41, No. 10, October 2013 (© 2013) pp. 2171–2180
DOI: 10.1007/s10439-013-0813-7

BMES BIOMEDICAL ENGINEERING SOCIETY™ www.bmes.org

Mechanics of the Mitral Annulus in Chronic Ischemic Cardiomyopathy

MANUEL K. RAUSCH,[1] FREDERICK A. TIBAYAN,[2] NEIL B. INGELS JR.,[3] D. CRAIG MILLER,[4] and ELLEN KUHL[1,4,5]

[1]Department of Mechanical Engineering, Stanford University, 496 Lomita Mall, Stanford, CA 94305, USA; [2]Department of Surgery, Oregon Health and Science University, Portland, OR 97239, USA; [3]Laboratory of Cardiovascular Physiology and Biophysics, Palo Alto Medical Foundation, Palo Alto, CA 94304, USA; [4]Department of Cardiothoracic Surgery, Stanford University, Stanford, CA 94305, USA; and [5]Department of Bioengineering, Stanford University, Stanford, CA 94305, USA

(*Received 1 March 2013; accepted 16 April 2013; published online 1 May 2013*)

Associate Editor Jane Grande-Allen oversaw the review of this article.

Abstract—Approximately one third of all patients undergoing open-heart surgery for repair of ischemic mitral regurgitation present with residual and recurrent mitral valve leakage upon follow up. A fundamental quantitative understanding of mitral valve remodeling following myocardial infarction may hold the key to improved medical devices and better treatment outcomes. Here we quantify mitral annular strains and curvature in nine sheep 5 ± 1 weeks after controlled inferior myocardial infarction of the left ventricle. We complement our marker-based mechanical analysis of the remodeling mitral valve by common clinical measures of annular geometry before and after the infarct. After 5 ± 1 weeks, the mitral annulus dilated in septal-lateral direction by 15.2% ($p = 0.003$) and in commissure-commissure direction by 14.2% ($p < 0.001$). The septal annulus dilated by 10.4% ($p = 0.013$) and the lateral annulus dilated by 18.4% ($p < 0.001$). Remarkably, in animals with large degree of mitral regurgitation and annular remodeling, the annulus dilated asymmetrically with larger distortions toward the lateral-posterior segment. Strain analysis revealed average tensile strains of 25% over most of the annulus with exception for the lateral-posterior segment, where tensile strains were 50% and higher. Annular dilation and peak strains were closely correlated to the degree of mitral regurgitation. A complementary relative curvature analysis revealed a homogenous curvature decrease associated with significant annular circularization. All curvature profiles displayed distinct points of peak curvature disturbing the overall homogenous pattern. These hinge points may be the mechanistic origin for the asymmetric annular deformation following inferior myocardial infarction. In the future, this new insight into the mechanism of asymmetric annular dilation may support improved device designs and possibly aid surgeons in reconstructing healthy annular geometry during mitral valve repair.

Keywords—Mitral annulus, Myocardial infarction, Ischemic mitral regurgitation, Strain, Curvature, Remodeling.

Address correspondence to Manuel K. Rausch, Department of Mechanical Engineering, Stanford University, 496 Lomita Mall, Stanford, CA 94305, USA Electronic mail: mkrausch@stanford.edu

INTRODUCTION

The mitral valve is one of four heart valves that ensure unidirectional blood flow through the heart into the pulmonary and systemic circulation. Located between the left atrium and the left ventricle, the open mitral valve enables efficient filling of the left ventricle with newly oxygenated blood before it closes to allow for proper ejection of the blood from the left ventricle into the aorta and eventually into the systemic circulation.[30]

Dysfunction of the mitral valve drastically reduces the efficiency of the heart and may be fatal, if untreated.[29] Numerous pathologies are known to affect mitral valve function; while some may cause excessive mitral valve narrowing, which impedes proper left ventricular filling, others may cause mitral valve leakage.[14,38] Leakage of the valve, also known as mitral regurgitation, may result either from disease to any of the mitral valve components, or from ventricular distortions that hinder mitral valve closure.[19] Ischemic disease of the left ventricle is known to be one of the causes for ventricular distortions that result in mitral regurgitation, also known as ischemic mitral regurgitation.[8]

Especially in the chronic setting, as the left ventricle remodels in response to myocardial necrosis and scarring, displacement of the postero-medial papillary muscle and of the myocardium surrounding the mitral valve may result in a force imbalance that initiates a remodeling process on the valvular level and demobilizes the mitral valve leaflets.[16,28] In particular, it is known that infarcts that include the postero-medial papillary muscle and the myocardium of the posterior wall cause dilation of the mitral annulus, especially in the septal-lateral direction, as well as asymmetric

dilation at the P3 segment. These changes, together with leaflet tethering, prevent proper leaflet coaptation and allow for blood to be ejected in the retrograde direction from the left ventricle back in the left atrium.[5,23,33]

While there are novel devices, techniques, and technologies under development to address ischemic mitral regurgitation, mitral valve repair with undersized annuloplasty rings remains the gold standard treatment option.[10,15,32] However, with one exception, most annuloplasty rings have not been developed specifically for the treatment of ischemic mitral regurgitation.[6] This may be one of the reasons for residual or recurrent mitral regurgitation in up to 30% of treated patients.[8,10,21] A deepened, quantitative understanding of the effects of ventricular remodeling on the mitral valve in the setting of ischemic mitral regurgitation could substantially improve current device designs and hopefully enhance treatment outcomes.

While previous studies have investigated the remodeling process of the mitral annulus using a wide array of technologies, none of these studies provides a quantitative, mechanical characterization of the changes in mitral valve kinematics.[11,18,35] The current manuscript aims to close this gap by providing maps of strain and curvature change along the entire mitral annulus between the healthy baseline heart and the chronic ischemic heart, in a well-established ovine model.[4,31,36,37] In particular, this manuscript tries to answer the questions: Which segments of the annulus are extended to cause annular dilation? Where along the annulus does the asymmetric distortion of the annulus originate? Does a mechanical analysis of the remodeling process support current annuloplasty ring designs?

METHODS AND MATERIALS

Animal Experiments

All animals received humane care in compliance with the Principles of Laboratory Animals Care formulated by the National Academy of Sciences and published by the National Institute of Health. This study is approved by the Stanford Medical Center Laboratory Research Animals Review Committee and conducted according to Stanford University policy.

Twenty-five Dorsett hybrid sheep (71 ± 5 kg) were premedicated with ketamine (25 mg/kg intramuscularly) and subsequently anesthetized intravenously with sodium thiopental (6.8 mg/kg IV). Throughout surgery, anesthesia was maintained with inhalational isoflurane (1% to 2.5%). Access to the heart was established *via* left thoracotomy. Polypropylene 2–0 sutures were snared around the second and third obtuse marginal branches of the left circumflex coronary artery. Once cardiopulmonary bypass was established and the heart was arrested, 17 markers were sewn to the mitral valve, eight to the annulus, five to the anterior leaflet, and four to the posterior leaflet, see Fig. 1. Left Ventricular (LV) pressure was measured using a micromanometer pressure transducer (PA4.5-X6, Konigsberg Instruments Inc., Pasadena, CA). Once the animals were taken off cardiopulmonary bypass, the tourniquets for the coronary artery snares were externalized through the fifth intercostal space and buried in a subcutaneous pocket. Due to respiratory complications four animals died during this procedure.

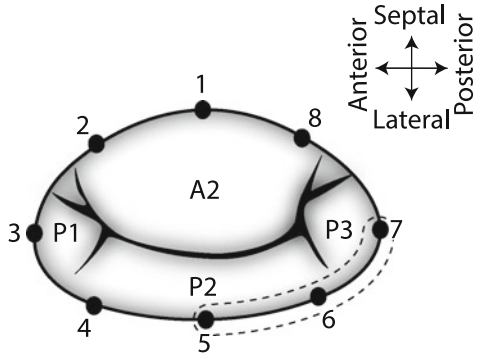

FIGURE 1. Schematic of the mitral valve with miniature markers 1–8. Individual posterior scallops are denoted P1–P3. The middle scallop of the anterior leaflet is denoted A2. The dashed outline of the lateral-posterior annulus indicates the location of the inferior infarct caused by ligation of the second and third obtuse marginal branches of the left circumflex artery.

Data Acquisition

After 8 ± 2 days, the animals were again taken to the cardiac catheterization laboratory and intravenously sedated with ketamine (1 to 4 mg/kg/h) and diazepam (5 mg). As before, sedation was maintained with inhalational isoflurane (1% to 2.5%). Under baseline conditions, during three consecutive cardiac cycles, marker locations were acquired *via* biplane videofluoroscopy (Philips Medical Systems, Pleasanton, CA). Videofluoroscopic images were taken in the right decubitus position at a sampling frequency of 60 Hz. Simultaneously, aortic pressure, LV pressure, and ECG signals were recorded. After the sheep were medicated with lidocaine (100 mg IV), bretylium (75 mg IV), and magnesium (3 g IV), coronary snares were tightened to occlude the second and third obtuse marginal branches of the left circumflex coronary artery. Complete vessel occlusion was verified *via* angiography. An epinephrine drip was titrated in order to maintain coronary perfusion pressure above 60 mmHg. Occurring ventricular arrhythmias were treated with lidocaine (50 to 100 mg IV) and amiodarone (50 to 150 mg IV). Due to refractory ventricular fibrillation, nine sheep died following coronary occlusion.

After 5 ± 1 weeks, the remaining animals returned to the cardiac catherization laboratory. Under chronic conditions, hemodynamic measurements and biplane videofluoroscopic recordings of marker coordinates were taken. Over the period of 5 ± 1 weeks, all but nine animals had lost significant markers, and were excluded from the study. The remaining group of $n = 9$ animals was selected as the final study group. Degree of mitral regurgitation was determined *via* transesophageal echocadiopgraphy, where regurgitant jet extent and width were evaluated in a three chamber view roughly equivalent to a vertical plane in humans.

Off-line, utilizing a semi-automated image processing and digitization software,[22] four-dimensional coordinates $\boldsymbol{\chi}_{\mathrm{n}}(t)$ for all n= $1,\ldots,8$ annular markers were obtained and stored for three consecutive heart beats, under both baseline condition and chronic condition. End diastolic time points were selected for all animals and each cardiac cycle as the time frames immediately before the rapid increase in left ventricular pressure indicating the beginning of the isovolumetric contraction.

Mathematical Model

As previously reported, from the eight four-dimensional marker coordinates $\boldsymbol{\chi}_{\mathrm{n}}(t)$, eight piecewise cubic Hermitian splines,

$$\boldsymbol{c}(s,t) = \sum_{i=0}^{3} b_{i,3}(s)\ \boldsymbol{\beta}_i(t), \tag{1}$$

were created and parameterized in terms of the arc length s, for every time point t of the three recorded cardiac cycles.[25] Here the Bernstein polynomials of degree three were defined as follows,

$$\begin{array}{ll} b_{0,3} = -s^3 + 3s^2 - 3s + 1 & b_{1,3} = 3s^3 - 6s^2 + 3s \\ b_{3,3} = s^3 & b_{2,3} = -3s^3 + 3s^2. \end{array} \tag{2}$$

The corresponding Bernstein coefficients,[24]

$$\begin{array}{lllllll} \boldsymbol{\beta}_0 & = & \boldsymbol{x}_0(t) & \boldsymbol{\beta}_1 & = & \boldsymbol{x}_0(t) & + \quad \boldsymbol{m}_0(t)/3 \\ \boldsymbol{\beta}_3 & = & \boldsymbol{x}_1(t) & \boldsymbol{\beta}_2 & = & \boldsymbol{x}_1(t) & - \quad \boldsymbol{m}_1(t)/3, \end{array} \tag{3}$$

were parameterized in terms of the positions $\boldsymbol{x}_0$, $\boldsymbol{x}_1$ and slopes $\boldsymbol{m}_0$, $\boldsymbol{m}_1$ at the beginning and end point of each spline segment. These coefficients $\boldsymbol{\beta}_i(t)$ were determined for each discrete time point t, by solving a least squares problem,

$$\sum_{\mathrm{n}=1}^{8} ||\boldsymbol{\chi}_{\mathrm{n}} - \boldsymbol{c}_{\mathrm{n}}(s,t)|| + \lambda \int_s ||\mathrm{d}_s^2 \boldsymbol{c}(s,t)||^2 \mathrm{d}s \rightarrow \min. \tag{4}$$

While the first term minimizes the distance from the markers positions $\boldsymbol{\chi}_{\mathrm{n}}$ to the spline curve $\boldsymbol{c}_{\mathrm{n}}(s,t)$, the second term minimizes the second derivative $\mathrm{d}_s^2 \boldsymbol{c}(s,t)$ of the overall spline, to enforce smoothness through the penalty parameter λ. Linear equality constraints were applied to ensure C^2-continuity.

Clinical Characterization

Common clinical measures of annular geometry are septal-lateral distance, commissure-commissure distance, mitral annular area, saddle-height, and septal and lateral perimeters. To characterize chronic geometric changes of the annulus, the above measures were calculated under baseline condition and chronic condition and compared. All clinical measures were calculated for three consecutive cardiac cycles and subsequently averaged as previously reported.[27]

Septal-lateral distance and commissure-commissure distance were calculated as the distances between the mid-septal and mid-lateral markers (markers 1 and 5), and between the anterior commissural and posterior commissural markers (markers 3 and 7), respectively. Mitral annular area was calculated as the area enclosed by the polygon spanned by projections of markers 1 through 8 onto the best fit plane through all annular markers. Saddle-height was defined as the average distance between the commissural markers and the mid-septal marker projected onto the normal to the best fit plane through all annular markers. Lastly, septal and lateral perimeters were calculated as the sums of the distances between the septal markers 8–2 and the lateral markers 2–8, respectively.

Mechanical Characterization

In addition to the above clinical measures, mechanical measures were calculated to compare the mechanics of the mitral annulus under baseline condition and chronic condition. In particular, strain and relative curvature were derived from the mathematical representation of the mitral annulus to quantify chronic alterations.

Strain is a measure of the relative displacement of continuum points along the annular perimeter between the reference time t_0 and the current time t. As a field quantity, strain allows us to identify, on a local level, where and to which extent the mitral annulus undergoes contraction and dilation during the transition from baseline to chronic condition. To analyze the deformation of the annulus between baseline condition and chronic condition, the baseline annulus at end diastole was chosen as the reference configuration (t_0) and the chronic annulus at end diastole was chosen as the current configuration (t).[2,3,26] The stretch $\lambda\,(s,\ t)$ was computed as the ratio between the lengths of the local tangent vectors in the current configuration $\mathrm{d}_s \boldsymbol{c}(s,t)$ and in the reference configuration $\mathrm{d}_s \boldsymbol{c}(s,t_0)$,

$$\lambda(s,t) = \mathrm{d}_s \boldsymbol{c}(s,t)/\mathrm{d}_s \boldsymbol{c}(s,t_0). \quad (5)$$

The stretch naturally defined the Green-Lagrange strain $E(s, t)$ along the annulus,

$$E(s,t) = \frac{1}{2}\left[\lambda^2 - 1\right] = \frac{1}{2}\left[\mathrm{d}_s \boldsymbol{c}(s,t)^2/\mathrm{d}_s \boldsymbol{c}(s,t_0)^2 - 1\right] \quad (6)$$

in terms of the local tangent vectors

$$\mathrm{d}_s \boldsymbol{c}(s,t) = \sum_{i=0}^{3} \mathrm{d}_s b_{i,3}(s)\, \boldsymbol{\beta}_i(t), \quad (7)$$

with the first derivatives of the Bernstein polynomials (2)

$$\begin{array}{ll} \mathrm{d}_s b_{0,3} = -3s^2 + 6s - 3 & \mathrm{d}_s b_{1,3} = 9s^2 - 12s + 3 \\ \mathrm{d}_s b_{3,3} = 3s^2 & \mathrm{d}_s b_{2,3} = -9s^2 + 6s \end{array} \quad (8)$$

and the coefficients $\boldsymbol{\beta}_i(t)$ determined from the minimization problem (4).

Absolute curvature is a measure of the deviation of a smooth curve from a straight line. Relative curvature is defined as the change in curvature a curve undergoes between two time points, the reference configuration t_0 and the current configuration t. It allows us to quantify the geometric changes the mitral annulus experiences during its transition from baseline condition to chronic condition.[7,17] Here, the absolute curvature κ (s, t) was calculated along the annulus at end diastole under baseline condition and chronic condition,

$$\kappa(s,t) = ||\mathrm{d}_s \boldsymbol{c}(s,t) \times \mathrm{d}_s^2 \boldsymbol{c}(s,t)||/||\mathrm{d}_s \boldsymbol{c}(s,t)||^3, \quad (9)$$

and the relative curvature $\Delta\kappa(s,t)$ was calculated as the difference between these two,

$$\Delta\kappa(s,t) = \kappa(s,t) - \kappa(s,t_0). \quad (10)$$

The second derivative

$$\mathrm{d}_s^2 \boldsymbol{c}(s,t) = \sum_{i=0}^{3} \mathrm{d}_s^2 b_{i,3}(s)\, \boldsymbol{\beta}_i(t) \quad (11)$$

was expressed in terms of the second derivatives of the Bernstein polynomials (2)

$$\begin{array}{ll} \mathrm{d}_s^2 b_{0,3} = -6s + 6 & \mathrm{d}_s^2 b_{1,3} = 18s - 12 \\ \mathrm{d}_s^2 b_{3,3} = 6s & \mathrm{d}_s^2 b_{2,3} = -18s + 6 \end{array} \quad (12)$$

and the coefficients $\boldsymbol{\beta}_i(t)$ from the minimization problem (4).

Similar to the clinical measures, strain and relative curvature fields were calculated for all three cardiac cycles and subsequently averaged. Furthermore, strain and relative curvature fields between baseline condition and chronic condition were quantified individually for each animal and averaged over all animals. To isolate the effects of annular remodeling from changes in myocardial contractility, all clinical and mechanical metrics were calculated at end diastole, where active contraction of the surrounding myocardium should be minimal.

Statistics

All data are reported as mean ± 1 standard deviation (SD). Hemodynamic data and clinical measures of annular geometry, recorded under baseline condition and chronic condition, were compared using the nonparametric Wilcoxon matched signed rank test. Statistical significance was defined for p-values below 0.05.

RESULTS

Marker coordinates were successfully recorded and digitized for all nine animals. Visual inspection revealed no apparent abnormalities in the marker data such as marker detachment or discontinuities in their temporal evolution.

Clinical Measures

Table 1 summarizes hemodynamic data for all animals under baseline and chronic conditions. Statistically significant difference was found only for heart rate (HR, $p < 0.05$), which dropped from baseline condition to chronic condition.

Table 2 shows the degree of mitral regurgitation under chronic condition for each animal. Of the nine animals, two developed severe mitral regurgitation of degree 4+, one moderate-severe of degree 3+, four moderate of degree 2+, and two mild of degree 1+.

Table 3 summarizes clinical measures of annular geometry calculated at end diastole under baseline condition, under chronic condition, and reported as percentage changes. Clinical measures of annular geometry reflect the significant remodeling on the valvular level following myocardial infarction. Septal-lateral distance increased significantly (15.2%, $p < 0.01$) as well as commissure-commissure distance (14.2%, $p < 0.005$). Consequently, mitral annular area during end diastole increased significantly as well (35.4%, $p < 0.005$). Mitral annular remodeling was also reflected in increases in septal and lateral perimeter. Interestingly, septal perimeter (10.4%, $p < 0.005$) increased less drastically than lateral perimeter (18.4%, $p < 0.005$). In contrast to previous measures, saddle height decreased following myocardial infarction. However, this change was not statistically significant.

TABLE 1. Hemodynamic summary (mean ± 1 standard deviation).

	Baseline	Chronic
HR*	107	85
(b/min)	±11	±9
LVP_{max}	95.4	81.2
(mmHg)	±12.9	±26.0
LVEDP	16.5	16.8
(mmHg)	±8.0	±8.8
dP/dt	1207.9	1006.1
(mmHg/s)	±725.9	±427.6
EDV	204.3	255.3
(ccm)	±125.8	±113.9
ESV	151.4	179.6
(ccm)	±110.9	±92.3

Shown are Heart Rate (HR), maximal Left Ventricular Pressure (LVPmax), Left Ventricular End Diastolic Pressure (LVEDP), dP/dt, End Diastolic Volume (EDV), and End Systolic Volume (ESV). Two-way paired Student *t* test was performed to compare hemodynamics between baseline condition and chronic condition. * indicates statistically significant difference between baseline condition and chronic condition with a *p*-value smaller than 0.05.

TABLE 2. Degree of Mitral Regurgitation (MR) under chronic condition. Mitral regurgitation was categorized as 0 (none-trace), 1+ (mild), 2+ (moderate), 3+ (moderate-severe), and 4+ (severe).

	Degree of MR	
Animal 1	severe MR	4+
Animal 2	moderate-severe MR	3+
Animal 3	severe MR	4+
Animal 4	mild MR	1+
Animal 5	moderate MR	2+
Animal 6	moderate MR	2+
Animal 7	moderate MR	2+
Animal 8	mild MR	1+
Animal 9	moderate MR	2+

Mechanical Measures

Spline representations for all nine annuli were successfully computed. The resulting approximating splines showed smooth contours and no apparent abnormalities, such as discontinuities. Approximation errors, i.e., distances between the original markers and the spline approximations, were checked and found to lie in the range of the acquisition error.

Strains along the mitral annuli of all nine animals between end diastole under baseline condition and chronic condition are illustrated in Fig. 2. The degree of annular remodeling in terms of strain varied across the nine animals. This inter-animal variation was also reflected in varying degree of mitral regurgitation reported in Table 1. However, across all animals, strains were predominantly positive, implying that the annuli were stretched from baseline condition to chronic condition. Quantitatively, peak strains for the individual animals ranged from 10 to 100%. On average, strains were smallest in the septal segment of the annulus, as low as 5%, and largest in the lateral segment, as high as 50%. The average location for peak strain was located in the lateral-posterior segment of the annulus.

TABLE 3. Mitral annular remodeling (mean ± 1 standard deviation).

	Baseline	Chronic	Change (%)
SL*	2.8	3.3	15.2
(cm)	±0.3	±0.3	
CC*	3.7	4.3	14.2
(cm)	±0.3	±0.3	
MAA*	7.8	10.6	35.4
(cm^2)	±1.4	±2.1	
SH	0.2	0.2	−6.4
(cm)	±0.2	±0.1	
SP*	3.2	3.6	10.4
(cm)	±0.5	±0.5	
LP*	7.4	8.7	18.4
(cm)	±0.7	±0.8	

Shown are Septal-Lateral (SL) distance, Commissure-Commissure (CC) distance, Mitral Annular Area (MAA), Saddle-Height (SH), Septal Annular Perimeter (SP), and Lateral Annular Perimeter (LP), under baseline condition and chronic condition at end diastole. Changes in clinical measures between baseline and chronic conditions represent as a measure of annular remodeling. * indicates a statistically significant difference between baseline condition and chronic condition with a p-value smaller than 0.05.

Furthermore, the spline representations of the individual annuli, black for baseline geometries and color-coded for chronic geometries, illustrate the geometric changes in mitral valve following myocardial infarction. While we found significant inter-animal variation, on average, we observed septal-lateral dilation and asymmetric deformation of the lateral-posterior segment of the annulus outlining the P3 segment. These characteristics were largely due to contributions from animals 1 and 3.

As an additional measure of annular mechanics, relative curvature between baseline condition and chronic condition at end diastole is shown, see Fig. 3. Relative curvature was predominantly negative, implying that the curvature decreased between baseline condition and chronic condition. All animals showed distinct points of localized peak relative curvature, differing significantly from the curvature of the remaining annulus.

DISCUSSION

Approximately 20–25% of the 6 million Americans that suffer from myocardial infarction also present with signs of ischemic mitral regurgitation.[6,19,39] With

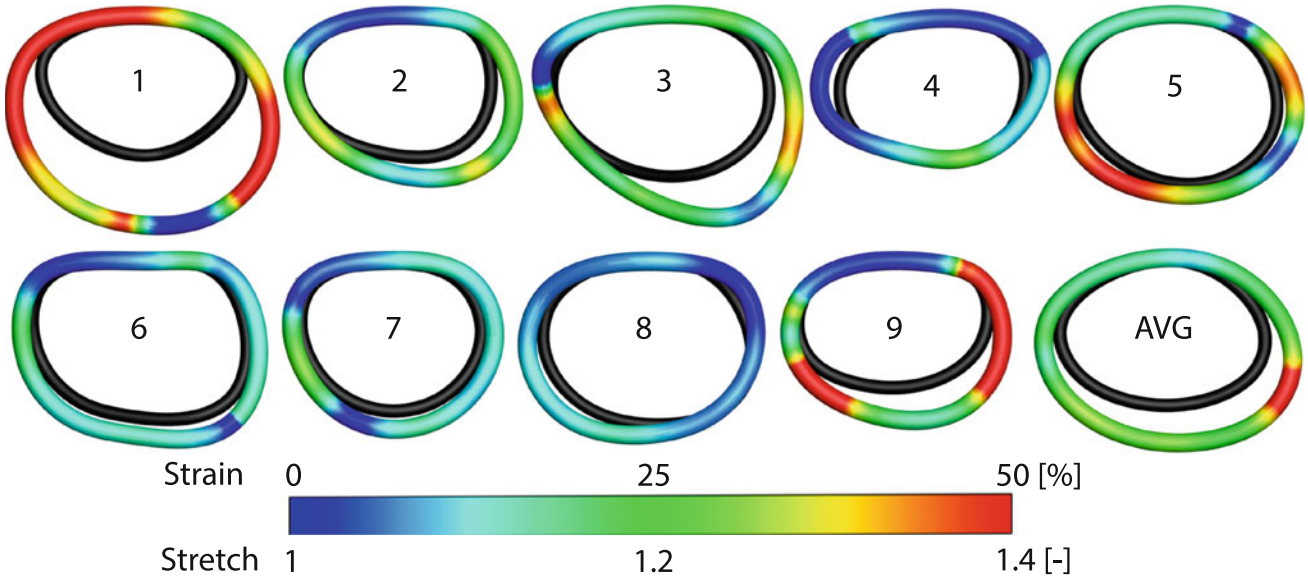

FIGURE 2. Mitral annular strain and stretch in the individual mitral annuli (animals 1–9) at end diastole between baseline condition (black) and chronic condition (color). Red represents tensile strain or stretch, while blue reveals no strain or stretch. The geometry, strain, and stretch along the annulus of the last image (AVG) were calculated as the average from all nine animals.

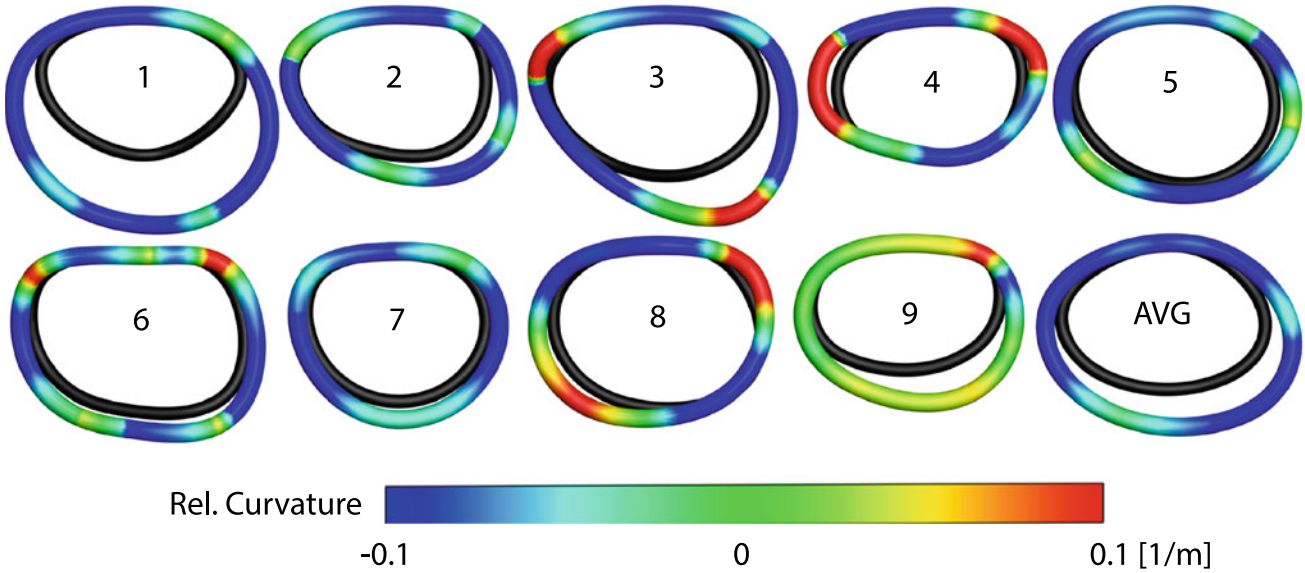

FIGURE 3. Mitral annular curvature alterations in the individual mitral annuli (animals 1–9) at end diastole between baseline condition (black) and chronic condition (color). Red illustrates an increase in curvature, while blue reveals a decrease in curvature. The geometry and the relative curvature along the annulus of the last image (AVG) were calculated as the average from all nine animals.

a rising prevalence of coronary heart disease in industrialized nations, the total number of patients with ischemic mitral regurgitation is expected to further increase in the future.[34] Now, more than ever, it is important to develop and device new treatments for ischemic mitral regurgitation based on an improved quantitative understanding of the effects of myocardial infarcts on mitral valve mechanics.

The current study presents a first mechanical analysis of mitral annular remodeling following myocardial infarction based on strain and curvature. Both fields were calculated at end diastole between the healthy baseline condition and chronic disease condition. In addition, classic clinical measures of mitral annular geometry, before and after the infarct, were computed to complement the mechanical analysis.

Clinical Measures

Results for clinical measures reflect the drastic changes the mitral valve is known to undergo in response to inferior myocardial infarction. Consistent with previous reports, the mitral annulus increased significantly in area, driven primarily by septal-lateral dilation and commissure-commissure dilation.[12] The most pronounced change in annular perimeter resulted from dilation of the lateral annulus, which had previously been identified as the primary cause of annular dilation in ischemic mitral regurgitation.[1] In accordance with previous studies, saddle-height did not undergo a statistically significant change at end diastole.[13] The degree of annular remodeling is closely correlated with the degree of mitral regurgitation. Animals with significant increase in septal-lateral dimension showed severe regurgitation, while animals with little to no such deformation showed only trace regurgitation. All other cases fell in between these extremes.

Mechanical Measures

The results of the mechanical analysis are in excellent agreement with previous studies. On average, we found markedly asymmetric infarct-induced dilation, largely due to the contributions of animals 1 and 3 with the most significant degree of mitral regurgitation and annular remodeling.[12] In these animals, largest distortions were found in the lateral-posterior direction, the location of myocardial infarct. Based on this observation, it may be hypothesized that remodeling of the infarcted myocardium and the surrounding tissue results in a local dilation. This dilation pulls the respective basal portion of the lateral-posterior wall away from the annulus, distorting the annulus in the course.

For the first time, we reported regionally varying strain fields that may provide further insight into the mechanistic origin of this dilation. The classical clinical measures already revealed that most annular dilation originated from the lateral rather than from the septal annulus. Strain and curvature fields confirmed that in the animals with significant degree of mitral regurgitation and annular dilation, large contributions to annular dilation stem from a highly localized section of the annulus closest to the P3 segment. Again, it seems that the remodeling myocardium perturbed the section of the annulus closest to the infarct, causing local strain peaks, twice as large as the strains in all other segments. Practically, this implies that the tangential forces, which deform the mitral annulus, are likely the largest in this segment. Therefore, the location closest to the infarct may be the region with the highest risk of ring dehiscence.[9]

FIGURE 4. Disease-specific annuloplasty ring for ischemic mitral regurgitation. A top view on the left shows the ring's characteristic features: an asymmetric outline with reduced curvature at the P3 segment and an increased sewing margin. The image on the right shows the same ring from a lateral perspective, with its characteristic dip close to the P3 segment. Photograph courtesy of Edwards Lifesciences.

Relative curvature plots revealed what has previously been described as circularization of the annulus following myocardial infarction.[18] Most of the annuli presented negative relative curvature. This implies that they increased in radius and, most obvious in the average representation, became less curved and more circular. However, relative curvature profiles displayed local interruptions to curvature homogeneity. Regions with high curvature may therefore be considered as hinge points for asymmetric distortion within the annular plane. This new insight could possibly aid surgeons to reversely identify and restore the healthy, non-infarcted geometry of the mitral annulus during mitral valve repair.

Clinical Significance

Undersized mitral valve annuloplasty is the gold standard treatment of ischemic mitral regurgitation.[10] Yet, 30% of all patients treated for ischemic mitral regurgitation present with residual or recurrent regurgitation upon follow up.[8,10,21] Clearly, current treatment strategies of ischemic mitral regurgitation are suboptimal. In response to this need, an annuloplasty ring was introduced to market with the specific goal of treating ischemic mitral regurgitation, see Fig. 4. According to the inventors, this ring incorporates an increased reduction in septal-lateral dimension relative to other, non-disease-specific annuloplastly rings. In addition, it possesses an asymmetric profile, with reduced P2–P3 curvature to accommodate the tethered P3 segment. An increased sewing margin additionally allows for a double suture row along the P2–P3 segment of the ring.[6]

Our mechanical analysis may provide some additional support for the design concept of this disease-specific annuloplasty ring. First, it illustrates a significant increase in septal-lateral dimension, which may be alleviated by the ring's aggressive downsizing. Second, the data clearly reveal an asymmetric dilation of the lateral-posterior segment in the animals that show the largest

degree of mitral regurgitation and annular remodeling. The ring's smaller curvature in this region may reduce the downsizing effect and thus limit the risk of damage to the surrounding tissue. Third, the ring's increased sewing margin, which allows for double suture rows, may provide the necessary support to prevent the large local strains from tearing the surrounding myocardial tissue and causing ring dehiscence.

Limitations

While this ovine model for chronic ischemic disease has been shown in the past to be highly repeatable, it is inherently different from human infarct patients. When extrapolating the knowledge gain from this study to human subjects, this limitation should be kept in mind. Furthermore, these sheep have undergone open heart surgery for maker placement before they were imaged in healthy and diseased conditions. It can therefore not be excluded that some of the mitral valve remodeling may be in response to open heart surgery and marker placement. Similarly, marker implantation itself may affect strain and curvature measurements. However, here we performed a simple quasi-static analysis and the weight of the individual markers was in the milligram range. It thus seems reasonable to assume that strain and curvature are affected only negligibly by marker implantation. Also, the duration of this study was 5 weeks on average. It may be possible that some aspects of mitral valve remodeling are initiated after a longer period of time and therefore were not visible in this analysis. Lastly, as reported in the result section of this manuscript, the quantitative analysis of each annulus revealed a large variation between the individual animals, especially in the diseased state. While baseline dimensions were similar between all animals, diseased mitral annuli differed largely both in size and in geometric distortion. One of the reasons for such large variation between animals may be inter-subject differences in coronary anatomy. These differences may result in varying infarct sizes and possibly varying infarct locations following the occlusion of obtuse marginal branches two and three.[11,20]

CONCLUSION

This is the first time that a quantitative, mechanical analysis provides additional insights into the mechanistic origins of asymmetric mitral annular dilation following inferior myocardial infarction. Our data illustrate that annular dilation in animals that present with large degree of mitral regurgitation and annular remodeling originates primarily from the lateral segment of the annulus; in particular from the lateral-posterior segment, where infarct-induced peak strains were 50% and higher. Annular dilation and peak strains were closely correlated to the degree of mitral regurgitation. The relative curvature analysis reveals the existence of distinct hinge points of localized curvature, from which this asymmetric distortion within the annular plane may originate. Overall, we believe that our combined clinical and mechanical analysis of mitral annular changes following inferior myocardial infarction provides additional understanding of disease-induced changes in the mitral valve. This new and mechanistic insight may support improved device designs and aid surgeons in reversely identifying healthy annular geometries during mitral valve repair.

ACKNOWLEDGEMENTS

We thank Paul Chang for technical assistance and Maggie Brophy for careful marker image digitization, and George T. Daughters III for computation of 4D data from biplane 2D marker coordinates. This work was supported by the Stanford Interdisciplinary Graduate Fellowship to Manuel K. Rausch, by US National Institutes of Health grants R01 HL29589 and R01 HL67025 to D. Craig Miller, and by the US National Science Foundation CAREER award CMMI 0952021 and INSPIRE grant 1233054 to Ellen Kuhl. None of the authors have a financial relationship to the products mentioned in this manuscript or any other conflict of interest.

REFERENCES

[1]Ahmad, R. M., A. M. Gillinov, P. M. McCarthy, E. H. Blackstone, C. Apperson-Hansen, J. X. Qin, D. Agler, T. Shiota, and D. M. Cosgrove. Annular geometry and motion in human ischemic mitral regurgitation: novel assessment with three-dimensional echocardiography and computer reconstruction. *Ann. Thorac. Surg.* 78:2063–2068, 2004.

[2]Amini, R., C. E. Eckert, K. Koomalsingh, J. McGarvey, M. Minakawa, J. H. Gorman, R. C. Gorman III, and M. S. Sacks. On the in vivo deformation of the mitral valve anterior leaflet: effects of annular geometry and referential configuration. *Ann. Biomed. Eng.* 40:1455–1467, 2012.

[3]Bothe, W., E. Kuhl, J. P. E. Kvitting, M. K. Rausch, S. Göktepe, J. C. Swanson, S. Farahmandnia, N. B. Ingels, Jr., and D. C. Miller. Rigid, complete annuloplasty rings increase anterior mitral leaflet strains in the normal beating ovine heart. *Circulation* 124:S81–S96, 2011.

[4]Bothe, W., M. K. Rausch, J. P. E. Kvitting, D. K. Echtner, M. Walther, N. B. Ingels Jr., E. Kuhl, and D. C. Miller. How do annuloplasty rings affect mitral annular strains in the normal beating ovine heart? *Circulation* 16:S231–S238, 2012.

[5]Carpentier, A. F., D. H. Adams, and F. Filsoufi. Carpentier's Reconstructive Valve Surgery. Elsevier Saunders, 2010.
[6]Daimon, M., S. Fukuda, D. H. Adams, P. M. McCarthy, A. M. Gillinov, A. Carpentier, F. Filsoufi, V. M. Abascal, V. H. Rigolin, S. Salzberg, A. Huskin, M. Langenfeld, and T. Shiota. Mitral valve repair with Carpentier-McCarthy-Adams IMR ETlogix annuloplasty ring for ischemic mitral regurgitation: early echocardiographic results from a multi-center study. *Circulation* 114:i588–i593, 2006.
[7]Eckert, C. E., B. Zubiate, M. Vergnat, J. H. Gorman, R. C. Gorman, and M. S. Sacks. In vivo dynamic deformation of the mitral valve annulus. *Ann. Biomed. Eng.* 37:1757–1771, 2009.
[8]Filsoufi, F., S. P. Salzber, and D. H. Adams. Current management of ischemic mitral regurgitation. *Mount Sinai J. Med.* 72:105–115, 2005.
[9]Gillinov, A. M., D. M. Cosgrove, B. W. Lytle, P. C. Taylor, R. W. Stewart, P. M. McCarthy, N. G. Smedira, D. D. Muehrcke, C. Apperson-Hansen, and F. D. Loop. Reoperation for failure of mitral valve repair. *J. Thorac. Cardiovasc. Surg.* 113:467–473, 1997.
[10]Gillinov, A. M., P. N. Wierup, E. H. Blackstone, E. S. Bishay, D. M. Cosgrove, J. White, B. W. Lytle, and P. M. McCarthy. Is repair preferable to replacement for ischemic mitral regurgitation?. *J. Thorac. Cardiovasc. Surg.* 122:1125-1141, 2001.
[11]Gorman, J. H. III., R. C. Gorman, T. Plappert, B. M. Jackson, Y. Hiramatsu, M. G. St John-Sutton, and L. H. Edmunds, Jr. Infarct size and location determine development of mitral regurgitation in the sheep model. *J. Thorac. Cardiovasc. Surg.* 115:615–622, 1998.
[12]Gorman, J. H. III, R. C. Gorman, B. M. Jackson, Y. Enomoto, M. G. St John-Sutton, and L. H. Edmunds, Jr. Annuloplasty ring selection for chronic ischemic mitral regurgitation: lessons from the ovine model. *Ann. Thorac. Surg.* 76:1556–1563, 2003.
[13]Gorman, J. H. III , B. M. Jackson, Y. Enomoto, and R. C. Gorman. The effect of regional ischemia on mitral valve annular saddle shape. *Ann. Thorac. Surg.* 77:544–548, 2004.
[14]Grande-Allen, K. J., J. E. Barber, K. M. Klatka, P. L. Houghtaling, I. Vesely, C. S. Moravec, and P. M. McCarthy. Mitral valve stiffening in end-stage heart failure: evidence of an organic contribution to functional mitral regurgitation. *J. Thorac. Cardiovasc. Surg.* 130: 783–790, 2005.
[15]Inoue, M., P. M. McCarthy, Z. B. Popovic, K. Doi, S. Schenk, H. Nemeh, Y. Ootaki, M. W. Kopcak, Jr., R. Dessoffy, J. D. Thomas, and K. Fukamachi. The Coapsys device to treat functional mitral regurgitation: in vivo long-term canine study. *J. Thorac Cardiovasc Surg.* 127:1068–1076, 2004.
[16]Kono, T., H. N. Sabbah, P. D. Stein, J. F. Brymer, and F. Khaja. Left ventricular shape as a determinant of functional mitral regurgitation in patients with severe heart failure secondary to either coronary artery disease or idiopathic dilated cardiomyopathy. *Am. J. Cardiol.* 68:355–359, 1991.
[17]Kvitting, J. P. E., W. Bothe, S. Göktepe, M. K. Rausch, J. C. Swanson, E. Kuhl, N. B. Ingels, and D. C. Miller. Anterior mitral leaflet curvature during the cardiac cycle in the normal ovine heart. *Circulation* 122:1683–1689, 2010. .
[18]Kwan, J., T. Shiota, D. A. Agler, Z. B. Popvic, J. X. Qin, M. A. Gillinov, W. J. Stewart, D. M. Cosgrove, P. M. McCarthy, and J. D. Thomas. Geometric differences of the mitral apparatus between ischemic and dilated cardiomyopathy with significant mitral regurgitation: real-time three-dimensional echocardiography study. *Circulation* 107:1135–1140, 2003. .
[19]Levine, R. A., J. Hung, Y. Otsuji, E. Messas, N. Liel-Cohen, N. Nathan, M. D. Handschumacher, J. L. Guerrero, S. He, A. P. Yoganathan, A. P. Vlahakes, and G. J. Vlahakes. Mechanistic insights into functional mitral regurgitation. *Curr. Cardiol. Rep.* 4:125–129, 2002.
[20]Llaneras, M. R., M. L. Nance, J. T. Streicher, J. A. Lima, J. S. Savino, D. K. Bogen, R. F. Deac, M. B. Ratcliffe, and L. H. Edmunds, Jr. Large animal model of ischemic mitral regurgitation. *Ann. Thorac. Surg* 57:432–439, 1994.
[21]McGee, E. C., A. M. Gillinov, E. H. Blackstone, J. Rajeswaran, G. Cohen, F. Najam, T. Shiota, J. F. Sabik, B.W. Lytle, P. M. McCarthy, and P.M. Cosgrove. Recurrent mitral regurgitation after annuloplasty for functional ischemic mitral regurgitation. *J. Thorac. Cardiovasc. Surg.* 128:916–924, 2004.
[22]Niczyporuk, M. A., and D. C. Miller. Automatic tracking and digitization of multiple radiopaque myocardial markers. *Comput. Biomed. Res.* 24:129–142, 1991.
[23]Rabbah, J. P., B. Chsim, A. Siefert, N. Saikrishnan, E. Veledar, V. H. Thourani, and A. P. Yoganathan. Effects of targeted papillary muscle relocation on mitral leaflet tenting and coaptation. *Ann. Thorac. Surg.* 95:621–628, 2012.
[24]Rajagopal, A., P. Fischer, E. Kuhl, and P. Steinmann. Natural element analysis of the Cahn-Hilliard phase-field model. *Comput. Mech.* 46:471–493, 2010.
[25]Rausch, M. K., W. Bothe, J. P. E. Kvitting, J. C. Swanson, N. B. Ingels, D. C. Miller, and E. Kuhl. Characterization of mitral valve annular dynamics in the beating heart. *Ann. Biomed. Eng.* 39:1690–1702, 2011.
[26]Rausch, M. K., W. Bothe, J. P. E. Kvitting, S. Göktepe, D. C. Miller, and E. Kuhl. In vivo dynamic strains of the ovine anterior mitral valve leaflet. *J. Biomech.* 44:1149–1157, 2011.
[27]Rausch, M. K., W. Bothe, J. P. E. Kvitting, J. C. Swanson, D. C. Miller, and E. Kuhl. Mitral valve annuloplasty: a quantitative clinical and mechanical comparison of different annuloplasty devices. *Ann. Biomed. Eng.* 40:750–776, 2012.
[28]Rausch, M. K., F. A. Tibayan, D. C. Miller, and E. Kuhl. Evidence of adaptive mitral leaflet growth. *J. Mech. Behav. Biomed. Mater.* 15:208–217, 2012.
[29]Rausch, M. K., N. Famaey, T. O'Brien Shultz, W. Bothe, D. C. Miller, and E. Kuhl. Mechanics of the mitral valve: a critical review, an in vivo parameter identification, and the effect of prestrain. *Biomech. Model. Mechanobiol.*. doi: 10.1007/s10237-012-0462-z, 2013.
[30]Sacks, M. S., and A. P. Yoganathan. Heart valve function: a biomechanical perspective. *Philos. Trans. R. Soc. B: Biol. Sci.* 363:1369–1391, 2007.
[31]Siefert, A. W., J. H. Jimenez, K. J. Koomalsingh, F. Aguel, D. S. West, T. Shuto, T. K. Snow, R. C. Gorman, J. H. Gorman III., and A. P. Yoganathan. Contractile mitral annular forces are reduced with ischemic mitral regurgitation. *J. Thorac. Cardiovasc. Surg.*. in press, 2012.
[32]Sündermann, S. H., M. Gessat, N. Cesarovic, T. Frauenfelder, P. Biaggi, D. Bettex, V. Falk, and S. Jacobs. Implantation of personalized, biocompatible mitral annuloplasty rings: feasibility study in an animal model. *Interact. Cardiovasc.Thorac. Surg.* 16:417–422, 2013.
[33]Szeto, W., R. C. Gorman, and J. H. Gorman III. Ischemic mitral regurgitation. In: Cardiac Surgery in the Adult,

edited by L. H. Cohn and L. H. Edmunds, Jr. New York, NY: McGraw-Hill, pp. 785–802, 2008.

[34]The American Heart Association Statistics Committee and Stroke Statistics Subcommittee. Executive Summary: Heart Disease and Stroke Statistics–2013 Update: A Report From the American Heart Association. *Circulation* 127:143–152, 2013.

[35]Tibayan, F. A., F. Rodriguez, M. K. Zasio, L. Bailey, D. Liang, G. T. Daughters, F. Langer, N. B. Ingels, Jr., and D.C. Miller. Geometric distortions of the mitral valvular-ventricular complex in chronic ischemic mitral regurgitation. *Circulation* 108(Suppl 1):II116–II121, 2003.

[36]Tibayan, F. A., F. Rodriguez, F. Langer, M. K. Zasio, L. Bailey, D. Liang, G. T. Daughters, N. B. Ingels Jr., and D. C. Miller. Annular remodeling in chronic ischemic mitral regurgitation: ring selection implications. *Ann. Thorac. Surg*. 76:1549–1554, 2003.

[37]Tibayan, F. A., F. Rodriguez, F. Langer, M. K. Zasio, L. Bailey, D. Liang, G. T. Daughters, M. Karlsson, N. B. Ingels, Jr., and D. C. Miller. Inreases in mitral leaflet radii of curvature with chronic ischemic mitral regurgitation.*J. Heart Valve Dis*. 13:772–778, 2004.

[38]Turi, Z. G. Mitral valve disease. *Circulation* 109:e38–e41, 2004.

[39]Wong, V. M., J. F. Wenk, Z. Zhang, G. Cheng, G. Acevedo-Bolton, M. Burger, D. A. Saloner, A. W. Wallace, J. M. Guccione, M. B. Ratcliffe, and L. Ge. The effect of mitral annuloplasty shape in ischemic mitral regurgitation: a finite element simulation. *Ann. Thoracic Surg*. 93: 776–782, 2012. .